JACS
JOURNAL OF THE AMERICAN CHEMICAL SOCIETY
Communication
pubs.acs.org/JACS

Spurious Observation of the Marcus Inverted Region in Bimolecular Photoinduced Electron Transfer

Arnulf Rosspeintner,[†] Marius Koch,[†] Gonzalo Angulo,[‡] and Eric Vauthey*[,†]

[†]Department of Physical Chemistry, University of Geneva, 30 Quai Ernest-Ansermet, 1211, Genève 4, Switzerland
[‡]Institute of Physical Chemistry, Polish Academy of Sciences, Kasprzaka 44/52, 01-224 Warsaw, Poland

Supporting Information

ABSTRACT: The effect of viscosity on the bimolecular electron transfer quenching of a series of coumarins by *N*,*N*-dimethylaniline was investigated using steady-state and time-resolved fluorescence spectroscopy. The data reveal that the static and transient stages of the quenching become dominant as viscosity increases. When extracting the quenching rate constants using a simple Stern−Volmer analysis, a decrease of the rate constant with increasing driving force is observed above ∼2 cP. However, this apparent Marcus inverted region, already reported several times with the same system in micelles and room temperature ionic liquids, totally vanishes when analyzing the data with a model accounting for the static and transient stages of the quenching. It appears that the apparent Marcus inverted region arises from the neglect of these quenching regimes together with the use of fluorophores with different excited-state lifetimes.

Since the seminal papers of Marcus on the theory of electron transfer (ET) reactions in liquids,[1] tremendous efforts have been invested to test the theoretical predictions, and to improve and refine the model. One of the most surprising predictions of the theory was the existence of the so-called Marcus Inverted Region (MIR) for highly exergonic ET. This effect, also predicted in the subsequent quantum-mechanical treatments,[2] had to wait for more than 20 years to be experimentally observed, first for intramolecular charge shift in radical cations and intramolecular charge recombination,[3] and later on for several other charge transfer processes.[4] However, the demonstration of the MIR for bimolecular photoinduced ET (BPET) proved to be much more difficult as, in most cases, the ET quenching rate constant increases with the driving force and then remains diffusion controlled even at very high exergonicity.[5] There have been several hypotheses to account for this deviation from theory, but none of them could be unambiguously verified.[5,6]

Over the past decade, however, there have been many reports of the observation of the MIR for BPET between a series of coumarins and *N*,*N*-dimethylaniline (DMA) in micelles and in room temperature ionic liquids (RTILs).[7] In all these cases, the quenching rate constants were extracted from the slope of Stern−Volmer (SV) plots of the average fluorescence lifetime versus quencher concentration. However, a SV analysis is only valid when the quenching occurs in the stationary regime. In fact, bimolecular ET quenching in solution comprises three stages:[8] the static, the nonstationary (transient), and the stationary quenching regimes, whose relative amplitudes depend on the medium viscosity and the quencher concentration. It has been recently shown that a simple SV analysis of the quenching, that is, a neglect of the static and nonstationary stages, leads to erroneous rate constants when working in viscous media and using fluorophores with an excited-state lifetime of a few nanoseconds.[9] As the above-mentioned observations of the MIR have been done in either viscous or constrained environments using chromophores with 1−6 ns fluorescence lifetimes, it is important to evaluate how the neglect of both static and nonstationary stages of the quenching in the data analysis impacts the driving-force dependence of the quenching rate constant and whether the MIR is not due to such a neglect.

To address these questions, we have investigated the effect of viscosity on the ET quenching by DMA of the same series of coumarins, for which the MIR has been reported, in acetonitrile (ACN), dimethylsulfoxide (DMSO), and two dimethylsulfoxide/glycerol mixtures (DMSO/GLY) (Chart 1).

The DMSO/GLY binary mixtures allow the viscosity to be varied without affecting the refractive index, the dielectric constant or the density.[12] The investigation was performed using both steady-state and time-resolved fluorescence. In the latter case, fluorescence up-conversion (FU) was used to measure the early stages of the quenching, whereas the slower quenching dynamics was recorded using time-correlated single photon counting (TCSPC).

With all coumarins investigated and in all solvents used, addition of DMA led to a decrease of the steady-state fluorescence intensity and to an acceleration of the fluorescence decay, due to an ET from DMA to the coumarins in the S_1 state. Figure 1 shows the strongly nonexponential time profiles of the fluorescence intensity measured in a 10 cP DMSO/GLY mixture at high DMA concentration. These measurements were recorded at a wavelength where the time profile of the fluorescence at early time without quencher is almost unaffected by the dynamic Stokes shift, ensuring that those depicted in Figure 1 mostly reflect the decay of the excited-state population. The nonexponential character of the fluorescence decays, that was also visible in the TCSPC measurements (Figure S2), is indicative of the occurrence of static and nonstationary quenching. Consequently, the sum of several

Received: May 21, 2012
Published: July 2, 2012

 © 2012 American Chemical Society dx.doi.org/10.1021/ja3049095 | *J. Am. Chem. Soc.* 2012, 134, 11396−11399

Chart 1. Structures and Properties (at 20 °C) of the Fluorophores, Quencher, and Solvents[a]

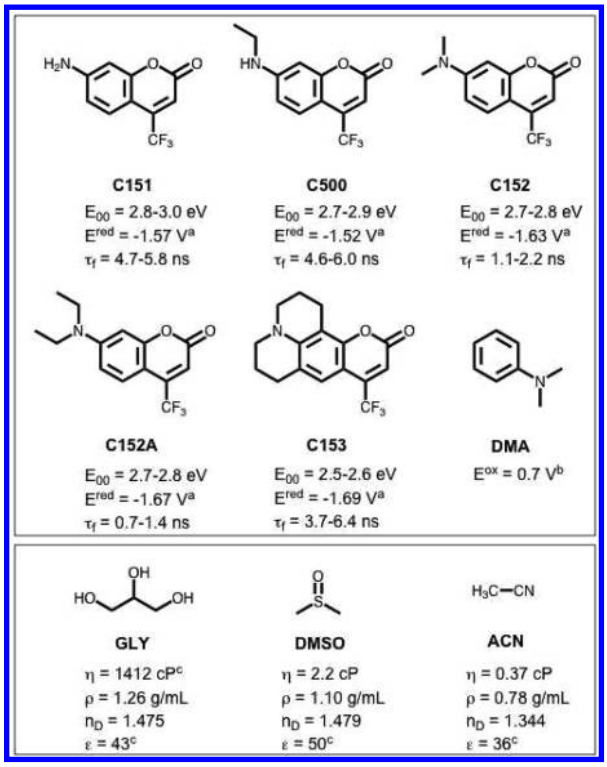

[a](a) From ref 7c, (b) from ref 10, (c) from ref 11.

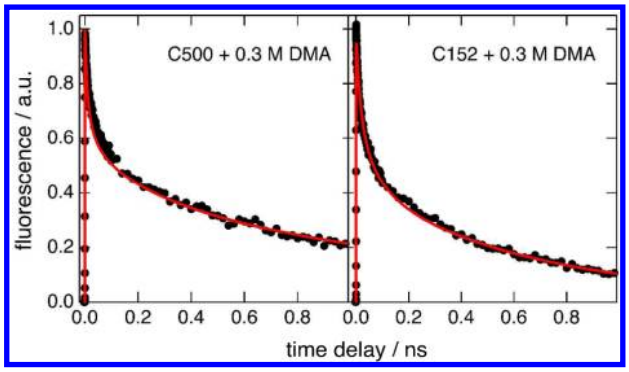

Figure 1. Fluorescence up-conversion profiles (black) measured with C500 and C152 in the presence of 0.3 M DMA in a 10 cP DMSO/GLY mixture. The red lines are the DET simulations.

exponential functions was used to properly reproduce the time profiles.

Lifetime SV plots were elaborated from the longest fluorescence decay time, τ_{long}, to minimize the contribution of the early quenching stages. Intensity SV plots were constructed from the steady-state fluorescence intensities. Whereas the lifetime plots were linear (Figure S4) and could be analyzed with eq 1a, the intensity plots were nonlinear in all solvents (Figure 2), indicative of the occurrence of static and nonstationary quenching. As a consequence, only the low concentration limit, where these two regimes are the smallest and the plots are linear, were analyzed using eq 1b:

$$\frac{\tau_f}{\tau_{long}(c)} = 1 + k_q^{\tau}\tau_f c; \qquad \frac{I_f(c=0)}{I_f(c)} = 1 + k_q^{s}\tau_f c \qquad (1a,b)$$

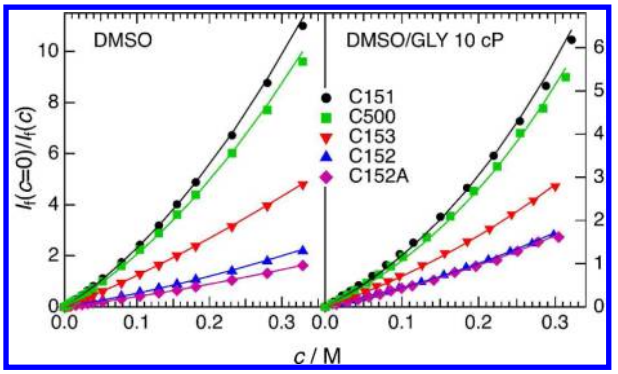

Figure 2. Steady-state intensity SV plots in DMSO and the 10 cP DMSO/GLY mixture (symbols) and best fits from DET (lines).

where c is the quencher concentration, k_q the quenching rate constant, τ_f the fluorescence lifetime without quencher and where the superscripts 'τ' or 's' denote that these values have been obtained from a lifetime or a steady-state intensity SV plot.

Figure 3 shows the variation of the quenching rate constants k_q^s with the driving force, estimated using the Weller equation

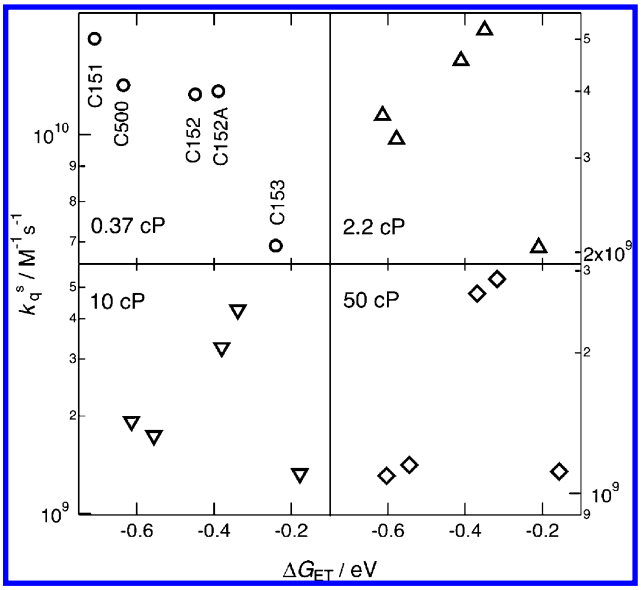

Figure 3. Effect of viscosity on the driving force dependence of the quenching rate constants k_q^s determined from eq 1a,b. The small variation of ΔG_{ET} from one solvent to another arises mainly from changes in the excited-state energy, E_{00}.

(eq. S14) and the values listed in Chart 1 and in Table S2. In ACN (0.37 cP), k_q^s increases with increasing driving force, as expected for ET quenching processes in this ΔG_{ET} range. However, as viscosity increases, an inversion of this behavior for the four more exergonic reactions appears and a bell-shaped dependence can be observed. This effect is the same as that reported previously and ascribed to the MIR.[7] There, the SV plots were constructed with either the steady-state intensity or the amplitude-averaged fluorescence lifetimes. Both types of plots are in principle totally equivalent, as long as no ultrafast fluorescence decay component has been overlooked. Figure 3 reveals that this inversion originates from a viscous environment only and does not require the ET to take place inside a micelle or in a RTIL.

dx.doi.org/10.1021/ja3049095 | J. Am. Chem. Soc. 2012, 134, 11396−11399

Two important points should be noted: (1) Whereas the k_q^s values in ACN are close to the diffusion rate constant $k_{diff} = 8 \times 10^6 RT/(3\eta) = 1.8 \times 10^{10}$ M^{-1} s^{-1}, where η is the viscosity in cP, those in the more viscous solvents are larger than k_{diff}, the difference increasing with viscosity. For example, $k_{diff} = 1.3 \times 10^8$ M^{-1} s^{-1} in the 50 cP mixture, whereas the k_q^s are 10−20 times as large. (2) The driving force dependence of k_q^τ exhibits an inversion effect as well, but only in the 10 and 50 cP mixtures (Figure S5). Moreover, the k_q^τ values depart less from k_{diff} than those of k_q^s.

These two observations suggest that, apart from those in ACN, the quenching rate constants obtained from the SV analysis do not correspond to the stationary rates and are 'contaminated' by the earlier stages of the quenching. To test this, we have analyzed the data with a model that accounts for all three quenching stages. We used the differential encounter theory (DET) that enables to combine a diffusion equation to determine the reactant pair distribution, $n(r,t)$, and Marcus theory to calculate the reaction probability at any distance, $w(r)$.[8d] In DET, the time dependence of the fluorescence intensity is given by:

$$I(t) = I(0) \exp\left[-\frac{t}{\tau_f} - c\int_0^t k(t')\,dt'\right] \quad (2)$$

where the quenching rate coefficient $k(t)$ is expressed as:

$$k(t) = 4\pi \int_{r=r_0}^{\infty} w(r) n(r,t) r^2\,dr \quad (3)$$

Figure 4 illustrates the effect of viscosity on the amplitude of these three quenching regimes calculated from eq 3. At early

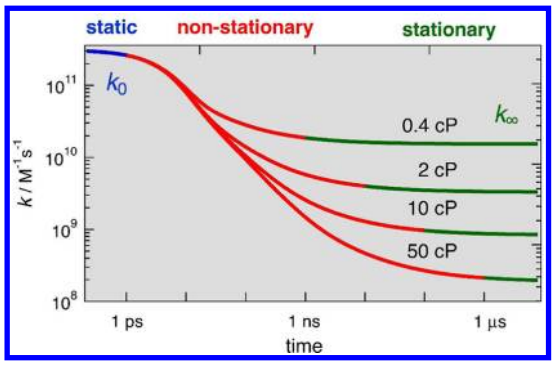

Figure 4. Effect of the viscosity of the medium on the quenching rates calculated from DET assuming solvent parameters similar to those of DMSO (except for viscosity), $\tau_f = 5$ ns, $\Delta G_{ET} = -0.5$ eV, and a contact radius of 7 Å.

time, quenching is static as it occurs between reactant pairs at optimal distance for ET. Consequently, the quenching rate is independent of viscosity and is equal to the intrinsic ET rate constant, k_0. At later times, quenching takes place between pairs at short but nonoptimal distance, and thus, some diffusive motion is required for ET. This nonstationary (transient) regime exists until the rate at which the pairs react is equal to the rate at which new reactive pairs are created by diffusion. This is the stationary stage, where quenching is diffusion controlled and its rate constant is equal to k_∞. In the nonstationary stage, the quenching rate decreases from k_0 to k_∞. As shown in Figure 4, both the duration and the amplitude of this stage, that is, the difference between k_0 and k_∞, increase dramatically with the viscosity of medium. The relative contributions of these three regimes to the fluorescence quenching also depend on the quencher concentration (eq 2). Therefore, both static and nonstationary regimes dominate at high quencher concentrations. On the other hand, the SV equation is only valid when the quenching is dominated by the stationary regime, that is, in low viscosity solvents and at low quencher concentration or when the electron transfer step itself is significantly slower than diffusion. In these cases, the quenching rate constant obtained from a SV analysis is close to k_∞.

Equation 2 was integrated to fit the steady-state SV plots as explained in detail in the Supporting Information. As illustrated in Figure 2, excellent agreement was obtained for all five coumarins in all four solvents with the parameters listed in Table S1. These parameters were also used to simulate the FU time profiles measured in the 10 cP mixture using eq 2. Very small adjustments of the parameters had to be done to perfectly reproduce the data, indicating that DET can describe consistently both time-resolved and steady-state quenching data. The resulting static and stationary quenching rate constants, k_0 and k_∞, are listed in Table S3 and represented as a function of ΔG_{ET} in Figure 5. The k_0 values exhibit two

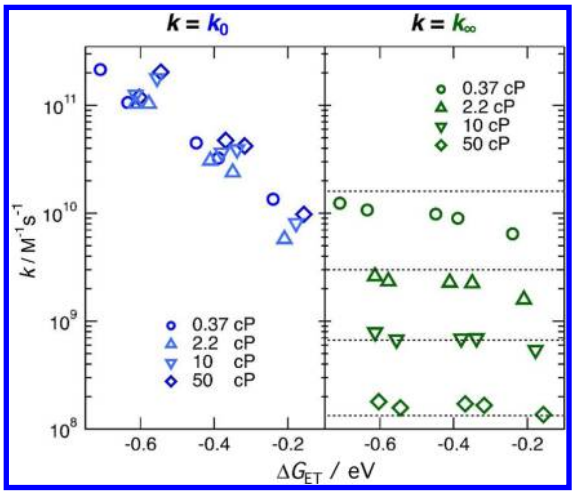

Figure 5. Quenching rates constant k_0 and k_∞ obtained from a DET analysis of the data (the dotted lines correspond to $k_{diff} = 8 \times 10^6 RT/(3\eta)$).

interesting features: (1) They are essentially the same for a given donor/acceptor pair and do not depend on solvent viscosity, in agreement with the static nature of the process reflected by these rate constants. (2) The inversion effect observed with k_q^s and k_q^τ is absent and, instead, k_0 increases with the driving force. Such behavior corresponds to the normal regime in Marcus theory and is that expected for this exergonicity range.[1b]

Essentially, the opposite behavior is observed with the stationary rate constants, k_∞: (1) They exhibit a strong solvent dependence, decreasing with increasing viscosity as expected for rate constants associated with diffusion. (2) For a given solvent, k_∞ is almost constant and independent of ΔG_{ET}. In fact, the slight variation of k_∞ is due to the increase of the quenching radius with driving force (Table S1). The dotted lines represent the values of k_{diff} calculated as discussed above and show that, in the stationary regime, the quenching is a diffusion-controlled process. Clearly, neither k_0 nor k_∞ exhibits a bell-shaped free energy dependence. In fact, comparison of

dx.doi.org/10.1021/ja3049095 | J. Am. Chem. Soc. 2012, 134, 11396−11399

Figures 3 and 5 reveals that the values obtained from a SV analysis in ACN coincide very well with k_∞, confirming that quenching at low quencher concentration in a low viscosity solvent is dominated by the stationary regime. On the other hand, the k_q^s and k_q^τ values in the more viscous solvents are all situated between k_0 and k_∞, confirming that these values are indeed contaminated by the early stages of the quenching. In such case, these k_q values do not have a real physical meaning.

The inversion of the k_q^s values in DMSO and higher viscosity media originates from the contribution of the static and nonstationary stages of the quenching that are not eliminated when performing a SV analysis at low quencher concentration. Figure 3 shows that the largest k_q^s values are always measured with C152 and C152A, that both have fluorescence lifetimes around 1 ns, whereas the other three coumarins have a 4−6 ns lifetime. Because of the time dependence of the quenching rate coefficient that extends well beyond 10 ns in viscous media (Figure 4), fluorophores with different excited-state lifetimes do not probe the same quenching regime. Indeed, a fluorophore with a short τ_f probes the early stages of the quenching and thus a SV analysis yields a k_q^s value closer to k_0 than to k_∞.[13] On the other hand, the longer the fluorescence lifetime, the closer to k_∞ is k_q^s. This is exactly what is happening here in DMSO and the DMSO/GLY mixtures. The inversion effect is simply due to the longer fluorescence lifetime of C151 and C500 compared to C152 and C152A. Therefore, these two fluorophores probe slower stages of the quenching than C152 and C152A. The resulting k_q^s values simply reflect the fluorescence lifetimes of the coumarins as demonstrated by Figure 6.

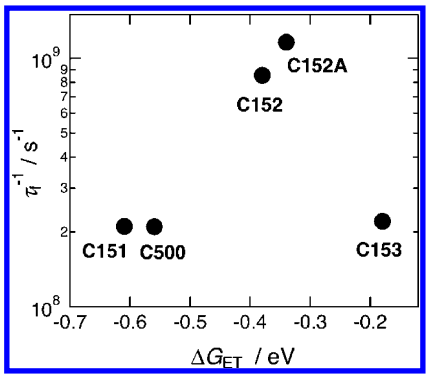

Figure 6. Inverse fluorescence lifetimes of the coumarins in DMSO/GLY at 10 cP as a function of the driving force for ET with DMA.

In conclusion, we have shown that the analysis of BPET quenching in viscous media requires the use of a model, like DET, that accounts for all stages of the quenching. Neglecting the contributions from static and dynamic quenching by performing a conventional SV analysis leads to quenching rate constants (i) between the static and the stationary rate constants and (ii) depending on the excited-state lifetime of the fluorophore. In the case of the coumarin series used here and in many other studies, this leads to an apparent decrease of the quenching rate constant with increasing driving force, that has been previously ascribed to the inverted region. However, the use of an adequate model yields rate constants that behave as expected for ET reactions in the weak to moderate range of driving force.

■ ASSOCIATED CONTENT

Supporting Information

Details about experiments and methods, data treatment and theoretical model. This material is available free of charge via the Internet at http://pubs.acs.org.

■ AUTHOR INFORMATION

Corresponding Author

Eric.Vauthey@unige.ch

Notes

The authors declare no competing financial interest.

■ ACKNOWLEDGMENTS

This work was supported by the University of Geneva and the Fonds National Suisse de la Recherche Scientifique through the NCCR MUST.

■ REFERENCES

(1) (a) Marcus, R. A. *Annu. Rev. Phys. Chem.* **1964**, *15*, 155. (b) Marcus, R. A.; Sutin, N. *Biochim. Biophys. Acta* **1985**, *811*, 265.
(2) Kestner, N. R.; Logan, J.; Jortner, J. *J. Phys. Chem.* **1974**, *78*, 2148.
(3) (a) Miller, J. R.; Calcaterra, L. T.; Closs, G. L. *J. Am. Chem. Soc.* **1984**, *106*, 3047. (b) Wasielewski, M. R.; Niemczyk, N. P.; Svec, W. A.; Pewitt, E. B. *J. Am. Chem. Soc.* **1985**, *107*, 1080.
(4) (a) Gould, I. R.; Ege, D.; Mattes, S. L.; Farid, S. *J. Am. Chem. Soc.* **1987**, *109*, 3794. (b) Guldi, D. M.; Asmus, K. D. *J. Am. Chem. Soc.* **1997**, *119*, 5744. (c) Vauthey, E. *J. Phys. Chem. A* **2001**, *105*, 340. (d) Mataga, N.; Chosrowjan, H.; Shibata, Y.; Yoshida, N.; Osuka, A.; Kikuzawa, T.; Okada, T. *J. Am. Chem. Soc.* **2001**, *123*, 12422.
(5) Rehm, D.; Weller, A. *Isr. J. Chem.* **1970**, *8*, 259.
(6) (a) Brunschwig, B. S.; Ehrenson, S.; Sutin, N. *J. Am. Chem. Soc.* **1984**, *106*, 6858. (b) Gladkikh, V.; Burshtein, A. I.; Angulo, G.; Pagès, S.; Lang, B.; Vauthey, E. *J. Phys. Chem. A* **2004**, *108*, 6667. (c) Rosspeintner, A.; Kattnig, D. R.; Angulo, G.; Landgraf, S.; Grampp, G. *Chem.—Eur. J.* **2008**, *14*, 6213.
(7) (a) Kumbhakar, M.; Mukherjee, T.; Pal, H. *Chem. Phys. Lett.* **2005**, *410*, 94. (b) Ghosh, S.; Mondal, S. K.; Sahu, K.; Bhattacharyya, K. *J. Chem. Phys.* **2007**, *126*, 204708. (c) Sarkar, S.; Pramanik, R.; Ghatak, C.; Rao, V. G.; Sarkar, N. *Chem. Phys. Lett.* **2011**, *506*, 211. (d) See the Supporting Information for a more comprehensive list of references.
(8) (a) Rice, S. A. *Comprehensive Chemical Kinetics, Vol 25. Diffusion Limited Reactions*; Elsevier: New York, 1985; (b) Murata, S.; Nishimura, M.; Matsuzaki, S. Y.; Tachiya, M. *Chem. Phys. Lett.* **1994**, *200*, 219. (c) Weidemaier, K.; Tavernier, H. L.; Swallen, S. F.; Fayer, M. D. *J. Phys. Chem. A* **1997**, *101*, 1887. (d) Burshtein, A. I. *Adv. Chem. Phys.* **2004**, *129*, 105.
(9) (a) Liang, M.; Kaintz, A.; Baker, G. A.; Maroncelli, M. *J. Phys. Chem. B* **2011**, *116*, 1370. (b) Koch, M.; Rosspeintner, A.; Angulo, G.; Vauthey, E. *J. Am. Chem. Soc.* **2012**, *134*, 3729.
(10) Morandeira, A.; Furstenberg, A.; Gumy, J. C.; Vauthey, E. *J. Phys. Chem. A* **2003**, *107*, 5375.
(11) Riddick, J. A.; Bunger, W. B. *Organic Solvents*; J. Wiley: New York, 1970.
(12) (a) Neufeld, A. A.; Burshtein, A. I.; Angulo, G.; Grampp, G. *J. Chem. Phys.* **2002**, *116*, 2472. (b) Angulo, G.; Kattnig, D. R.; Rosspeintner, A.; Grampp, G.; Vauthey, E. *Chem.—Eur. J.* **2010**, *16*, 2291.
(13) Burshtein, A. I.; Sivachenko, A. Y. *J. Photochem. Photobiol., A* **1997**, *109*, 1.